A MODEL PREDICTIVE CONTROL ALGORITHM FOR THE FORMATION CONTROL OF NANOSATELLITES IN LEO ORBIT

Caterina Santoro[1], Salvatore Rosario Bassolillo[2], Alessia Ferraro[3], Luciano Blasi[1] & Immacolata Notaro[1]

[1]Department of Engineering, University of Campania Luigi Vanvitelli, 81031, Aversa (CE), Italy
[2]Department of Science and Technology, University of Naples Parthenope, 80143, Napoli, Italy
[3]Dipartimento di Ingegneria DIIES, Univ. "Mediterranea" of Reggio Calabria, Reggio Calabria, Italy

Abstract

This paper deals with the formation flight control of Cubesat-type nanosatellites in Low Earth Orbit (LEO), employing a decentralized model predictive control algorithm aimed at minimizing tracking error. The proposed technique's effectiveness has been proved through numerical simulations, using a non-linear simulator taking into account the effects of atmospheric drag, and gravitational field variations as a function of latitude and longitude.

Keywords: Cubesat, Model Predictive Control (MPC), Satellite Formation,

1. General Introduction

In recent years, the concept of formation flight (FF) has garnered significant attention in the aerospace community [1, 2]. This interest arises from the potential benefits of FF, such as cost-effectiveness, improved performance, and enhanced adaptability compared to individual spacecraft [3]. Allocating various functions and payloads across a synchronized fleet of spacecraft has the potential to improve mission science outcomes. In addition, the use of a network of cooperating satellites increases redundancy in the event of failures.

A Satellite Formation Flight (SFF) can be defined as the coordinated motion of multiple spacecraft whose dynamic states are interlinked by a common control law. Solutions to the SFF control problem can be broadly classified into Multiple-Input Multiple-Output (MIMO) approaches, Leader-Follower (LF) schemes, Virtual Structure (VS) schemes, Cyclic techniques, and Behavioral methods [4, 3].

In the MIMO scheme, the formation dynamics are treated as a large MIMO system, employing advanced control methods to achieve optimality and stability. However, this demands a high degree of communication between agents [5]. The LF scheme simplifies control into individual tracking problems with a strict hierarchy, applicable to trailing and clustered configurations, the latter being a particular structural type of formation. In the VS approach, the goal is to mimic the behaviour of objects in a rigid structure, defining two types of virtual structures: Iterated Virtual Structures (IVS) and Guidance Virtual Structures (GVS) [6]. The cyclic approach is similar to LF but without the hierarchical constraint, allowing two spacecraft to provide feedback via their relative state [7]. Behavioural methods combine multiple controllers for various behaviours, with formation control being one essential behaviour. Behavioural control is an extension of one or more control methods [4].

This paper is focused on the FF of Cubesat-type nanosatellites in Low Earth Orbit (LEO). Cubesats, being small satellites used for various applications [8], face challenges in autonomy, failure resilience, and position and attitude control when deployed in LEO. Environmental disturbances such as drag, solar pressure, and J2 current anomalies [9] pose threats to the formation integrity, necessitating robust response mechanisms. The limitations inherent in Cubesats, such as restricted sensors, onboard computing, communication bandwidth, and propulsion capacity, make the design of a formation

control algorithm challenging. In particular, the lack of suitable propulsion systems in Cubesats represents a major challenge in the design of a formation control algorithm, with only a few missions such as IMPACT and BricSAT-P featuring electrospray thrusters and micro-cathode arc thrusters, respectively [10].
In recent years, advancements in electric micro-propulsion have enhanced fuel efficiency and miniaturization, making it suitable for Cubesats [11]. This study focuses on n nano-satellites of the Cubesat type in Low Earth Orbit (LEO), forming a Satellite Formation Flight (SFF) mission. The formation control algorithm is employed to modify, sustain, or initially establish the satellite formation. Each CubeSat propulsion system comprises six cold thrusters positioned along the positive and negative axes of the satellite's body. The architecture can be viewed as virtual, incorporating a different thruster configuration and suitable control allocation [12, 13].
A receding horizon control method, widely used over the years to manage the presence of constraints and nonlinearities typical of FF [14, 15, 16], was developed to optimize both trajectory tracking and consumption while maintaining the formation in an almost rigid structure, taking into account thruster constraints and performance, and leveraging the potential of efficient trajectory planning algorithms onboard [17, 18, 19].
Numerical simulations prove the effectiveness of the proposed control algorithm, which allows for maintaining a small tracking error in the presence of typical perturbations of LEO orbits with a reasonable control effort.

2. Model Predictive Control

According to the receding horizon approach, at each time step k, the Model Predictive Control (MPC) solves a constrained optimization problem to determine an optimal control sequence $\boldsymbol{U}(k) = \left[\boldsymbol{u}(k|k)^T, \boldsymbol{u}(k+1|k)^T ... \boldsymbol{u}(k+N|k)^T\right]^T$ within a given prediction time horizon, $[t_k, t_k + NT_c]$, where N is the number of time steps and T_c is the sample time. However, only the first move $\boldsymbol{u}^*(k|k)$ is applied to the plant.
The optimization problem aims to minimize a cost function $J(\boldsymbol{\xi}(k|k), \boldsymbol{U}(k), k)$, considering the tracking error and the control effort in the prediction time horizon by evaluating the future system behaviour. A quadratic cost function is adopted:

$$\begin{aligned} J(\boldsymbol{\xi}(k|k), \boldsymbol{U}(k), k) = \\ = \sum_{i=0}^{N} \left(\boldsymbol{\xi}(k+i|k) - \overline{\boldsymbol{\xi}}(k+i)\right)^T \boldsymbol{Q} \left(\boldsymbol{\xi}(k+i|k) - \overline{\boldsymbol{\xi}}(k+i)\right) + \\ + \boldsymbol{u}(k+i|k)^T \boldsymbol{R} \boldsymbol{u}(k+i|k) + \\ + \left(\boldsymbol{\xi}(k+N+1|k) - \overline{\boldsymbol{\xi}}(k+N+1)\right)^T \boldsymbol{S} \left(\boldsymbol{\xi}(k+N+1|k) - \overline{\boldsymbol{\xi}}(k+N+1)\right) \end{aligned} \tag{1}$$

where

- $\left(\boldsymbol{\xi}(k+i|k) - \overline{\boldsymbol{\xi}}(k+i)\right)^T \boldsymbol{Q} \left(\boldsymbol{\xi}(k+i|k) - \overline{\boldsymbol{\xi}}(k+i)\right)$, measures the state deviation from a desired state vector $\overline{\boldsymbol{\xi}}(k+i)$,
- $\boldsymbol{u}(k+i|k)^T \boldsymbol{R} \boldsymbol{u}(k+i|k)$, accounts for the control authority,
- $\left(\boldsymbol{\xi}(k+N+1|k) - \overline{\boldsymbol{\xi}}(k+N+1)\right)^T \boldsymbol{S} \left(\boldsymbol{\xi}(k+N+1|k) - \overline{\boldsymbol{\xi}}(k+N+1)\right)$, weights the terminal tracking error.

The weight matrices $\boldsymbol{Q}$ and $\boldsymbol{S}$ are assumed semidefinite positive, while $\boldsymbol{R}$ is positive definite.
The optimization problem's constraints include the prediction model to account for the future plant behaviour (2) as well as the limitations on states, outputs, and control variables (4):

$$\boldsymbol{\xi}(k+i+1|k) = \boldsymbol{A_d}\boldsymbol{\xi}(k+i|k) + \boldsymbol{B_d}\boldsymbol{u}(k+i|k) \, \forall i = 0, 1, ..., N \tag{2}$$

$$\boldsymbol{\xi}(k|k) = \boldsymbol{\xi}(k) \tag{3}$$

$$\boldsymbol{g}(\boldsymbol{\xi}(k|k), \boldsymbol{U}(k), k) \leq 0 \tag{4}$$

To facilitate the Quadratic Programming solver, the constraints in (4) are formulated as linear inequalities:

$$\begin{array}{c} \boldsymbol{\xi}_m \leq \boldsymbol{\xi}\,(k+i+1|k) \leq \boldsymbol{\xi}_M \\ u_m \leq u\,(k+i|k) \leq u_M \qquad \forall i = 0, 1, ..., N \end{array} \tag{5}$$

where $\boldsymbol{\xi}_m$ and $\boldsymbol{\xi}_M$ denote the lower and upper bounds for the state $\boldsymbol{\xi}(\cdot)$, whereas $\boldsymbol{u}_m$ and $\boldsymbol{u}_M$ set the limits of the input vector $\boldsymbol{u}(\cdot)$.

3. Satellite Formation Model: Hill-Clohessy-Wiltshire equations

The Hill-Clohessy-Wiltshire (HCW) equations offer a simplified model for relative orbital motion, where a leader satellite is in a circular orbit and a follower spacecraft is in either an elliptical or circular orbit. Consider the local vertical local horizontal (LVLH) reference frame, centred in the centre of mass of the leader satellite, with the x-axis aligned with the radius vector, the y-axis running parallel to the tangent of the Reference Orbit, and the z-axis forming a right-handed system. Assumptions include:

(i) The leader satellite is in a constant circular orbit with angular velocity $\varpi = \sqrt{(GM_E)/r^3}$, where G is the gravitational constant, and M_E is the Earth's mass.

(ii) The relative distance between the leader and follower satellites is significantly smaller than the leader satellite's distance from the Earth's centre.

(iii) No external disturbances act on the satellite.

The HCW equations for relative motion are given by [20, 21]:

$$\begin{aligned} \ddot{x} &= 3\varpi^2 x + 2\varpi\dot{y} + a_x \\ \ddot{y} &= -\varpi\dot{x} + a_y \\ \ddot{z} &= -\varpi^2 z + a_z \end{aligned} \tag{6}$$

These equations can be expressed in matrix form as:

$$\dot{\boldsymbol{\xi}} = \boldsymbol{A}\boldsymbol{\xi} + \boldsymbol{B}\boldsymbol{u} \tag{7}$$

where $\boldsymbol{\xi} = [x, y, z, \dot{x}, \dot{y}, \dot{z}]^T$ is the state vector (position and velocity), and $\boldsymbol{u} = [a_x, a_y, a_z]^T$ is the input vector. The state matrix $\boldsymbol{A}$ and the input matrix $\boldsymbol{B}$ are given by:

$$\begin{aligned} \boldsymbol{A} &= \begin{bmatrix} 0 & 0 & 0 & 1 & 0 & 0 \\ 0 & 0 & 0 & 0 & 1 & 0 \\ 0 & 0 & 0 & 0 & 0 & 1 \\ 3\varpi^2 & 0 & 0 & 0 & 2\varpi & 0 \\ 0 & 0 & 0 & -2\varpi & 0 & 0 \\ 0 & 0 & -\varpi^2 & -0 & 0 & 0 \end{bmatrix} \\ \boldsymbol{B} &= \begin{bmatrix} 0 & 0 & 0 \\ 0 & 0 & 0 \\ 0 & 0 & 0 \\ 1 & 0 & 0 \\ 0 & 1 & 0 \\ 0 & 0 & 1 \end{bmatrix} \end{aligned} \tag{8}$$

Consider the sample time T_c as the control algorithm execution time. The mathematical model described by (7) and (8) is converted into a suitable discrete-time set of state equations as follows:

$$\boldsymbol{\xi}(k+1) = \boldsymbol{A}_d\boldsymbol{\xi}(k) + \boldsymbol{B}_d\boldsymbol{u}(k) \tag{9}$$

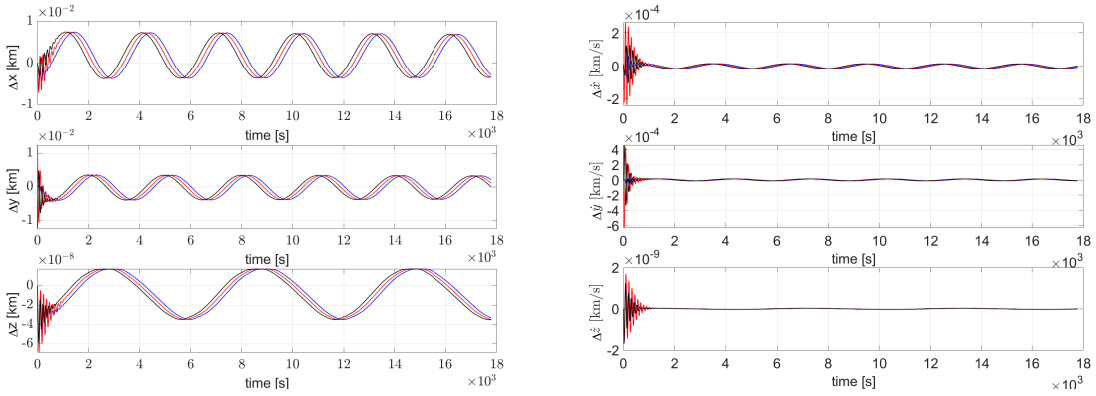

(a) (b)

Figure 1 – Tracking error. Curves for satellite #1, #2, and #3 are depicted with blue, red, and black lines, respectively. (a) Position error. (b) Velocity error.

$$\begin{aligned} \boldsymbol{A}_d &= e^{\boldsymbol{A}T_c} \\ \boldsymbol{B}_d &= \int_0^{T_c} e^{\boldsymbol{A}(t-\tau)} \boldsymbol{B} d\tau \end{aligned} \tag{10}$$

where $\boldsymbol{\xi}(k) = [x(k), y(k), z(k), \dot{x}(k), \dot{y}(k), \dot{z}(k)]^T$ and $\boldsymbol{u}(k) = [a_x(k), a_y(k), a_z(k)]^T$ are the state and the input vectors at time instant k, whereas $\boldsymbol{A}_d$ and $\boldsymbol{B}_d$ are the discrete-time state and input matrices.

4. Numerical results

A numerical simulation campaign was carried out to test the performance of the proposed controller. In the following, we present a test case in which three satellites have to guarantee an assigned formation, achieving a tandem configuration where each satellite maintains a constant distance from the preceding satellite.

Every satellite is controlled using the MPC algorithm, whose prediction model is based on HCW equations (9) and (10). Consequently, satellite #1 follows a virtual leader (VL), tracking an unperturbed reference trajectory, whereas satellite #2 has to maintain a constant distance from satellite #1. The same, satellite #3 follows satellite #2, preserving the desired mutual anomaly.

In Table 1, the simulation parameters are resumed. It is assumed that the satellites maintain, during their orbits, a difference in true anomaly of $10deg$, starting with a slight tracking error, defined in terms of a true anomaly of $0.001deg$.

To take into account realistic parameters, the formation is composed by three 3U Cubesats of mass equal to $4kg$. The propulsion system of each CubeSat consists of six different cold thrusters, arranged along the positive and negative axes of the satellite body. Each thruster can generate a maximum acceleration of $1.25\,m/s^2$.

The dynamics of each satellite is described by a non-linear 6DoF model [22], including the effects of the atmospheric drag and the zonal harmonic J_2. Each satellite is equipped with an attitude controller that allows it to maintain a constant orientation relative to the local tangent plane.

Figure 1 shows the tracking errors, $\boldsymbol{\Delta\xi}(k) = \boldsymbol{\xi}(k) - \bar{\boldsymbol{\xi}}(k)$ of each satellite with respect to its own leader, whereas in Figure 2, the resulting control signals are illustrated.

It is worth noting that, at the beginning of the simulation, the positions of satellite #2 and satellite #3 differ from the desired ones, consequently, the initial value of the acceleration provided by the controller is not equal to zero.

Figure 3 shows the relative distance between each satellite and its respective leader. After a small transient phase, due to the initial position error of satellites #2 and #3, the mutual distance between each couple of satellites is always below $1 \times 10^{-2} km$, also in the presence of $J2$ and drag effects.

Furthermore, the shape of the formation is maintained during the orbit, as depicted in Figure 4, where the position of the satellites $[x, y, z]^T$, in the LVLH reference frame, is shown.

Table 1 – Test-case with three satellites: analysis data.

Orbital Elements	Satellite #1
Semimajor axis	7078.4 km
Eccentricity	0
Inclination	90 deg
Longitude of the ascending node	0 deg
Argument of periapsis (deg)	0
True anomaly (deg)	0.0 deg
Control objective	Track an unperturbed trajectory
Desired mutual distances from its leader	0
Orbital Elements	**Satellite #2**
Semimajor axis	7078.4 km
Eccentricity	0
Inclination	90 deg
Longitude of the ascending node	0 deg
Argument of periapsis	0 deg
True anomaly	10.001 deg
Control objective	Follow Satellite #1
Desired mutual anomaly from its leader	10.0 deg
Orbital Elements	**Satellite #3**
Semimajor axis	7078.4 km
Eccentricity	0
Inclination	90 deg
Longitude of the ascending node	0 deg
Argument of periapsis	0 deg
True anomaly	20.001 deg
Control objective	Follow Satellite #2
Desired mutual anomaly from its leader	10.0 deg

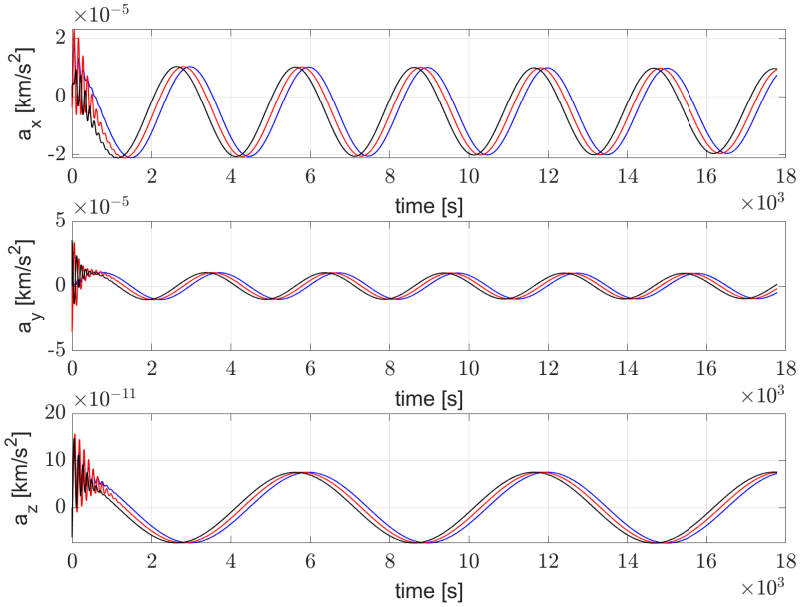

Figure 2 – MPC controlled acceleration. Curves for satellite #1, #2, and #3 are depicted with blue, red, and black lines, respectively.

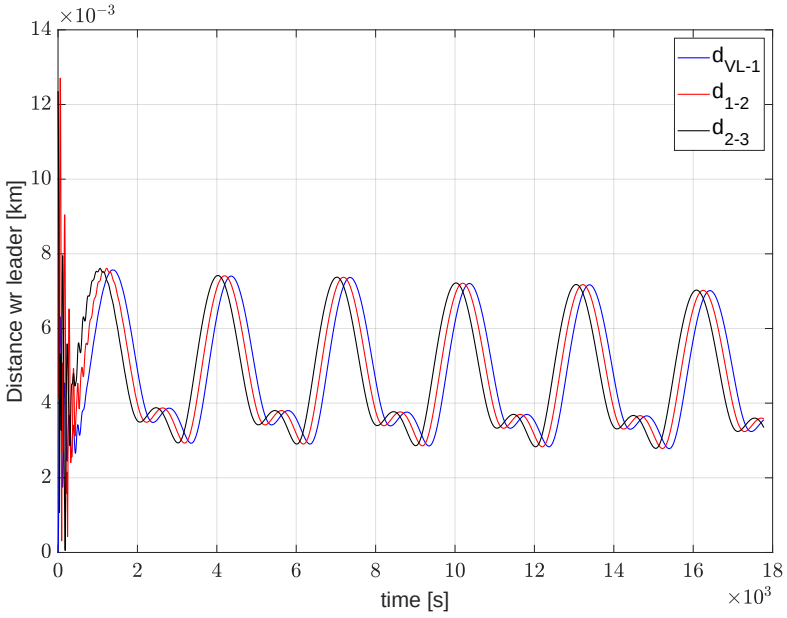

Figure 3 – Relative distance between each satellite and its respective leader. Blue, red, and black lines represent, respectively, the distance of Satellite #1 with respect to Virtual Leader (VL), the distance of Satellite #2 with respect to Satellite #1, and the distance of Satellite #3 with respect to Satellite #2.

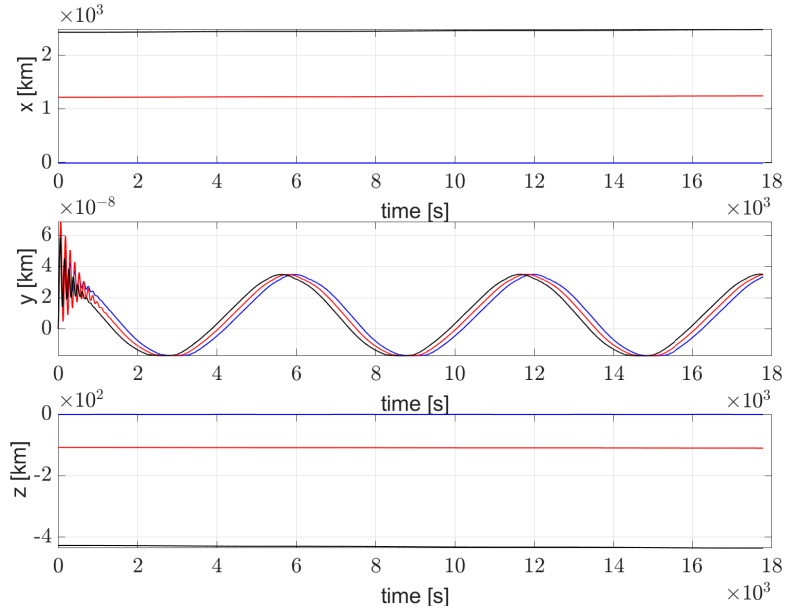

Figure 4 – Satellite position with respect to Virtual Leader (VL) in LVLH frame. Blue, red, and black lines represent, respectively, position of Satellite #1, #2, and #3.

5. Conclusions

In this paper, the design and testing of a flight control scheme based on a decentralized MPC algorithm for a formation of Cubesat-type nanosatellites in LEO orbit is presented. In particular, the main aim of the flight control algorithm is to minimize the tracking error while considering the minimization of thruster activation. To prove the effectiveness of the proposed methodology, a realistic test-case has been carried out on a non-linear simulator, taking into account disturbances due to atmosphere drag, and gravitational field variations as a function of latitude and longitude. The simulated scenario considered the tracking of a reference trajectory by a formation consisting of three satellites orbiting in LEO orbit. In particular, the proposed architecture shows the capability to ensure an effective tracking of the reference trajectory, maintaining the formation shape during the simulation while effectively avoiding collisions between the satellites.

6. Contact Author Email Address

For any further information, mail to: immacolata.notaro@unicampania.it

7. Copyright Statement

8. Acknowledgement

This work was supported by the research project - ID:20222N4C8E "Resilient and Secure Networked Multivehicle Systems in Adversary Environments" granted by the Italian Ministry of University and Research (MUR) within the PRIN 2022 program, funded by the European Union through the PNRR program.

References

[1] K. Schillinga, G. Loureirob, Y. Zhangc, A. Nüchtera, J. Scharnagld, I. Motroniukd, and A. Aumannd, "Tim: An international nano-satellite formation for photogrammetric earth observation," in *70th International Astronautical Congress (IAC), Washington D.C., United States*, 2019.

[2] A. Freimann, T. Petermann, and K. Schilling, "Interference-free contact plan design for wireless communication in space-terrestrial networks," in *2019 IEEE International Conference on Space Mission Challenges for Information Technology (SMC-IT)*, pp. 55–61, IEEE, 2019.

[3] B. Andrievsky, A. M. Popov, I. Kostin, and J. Fadeeva, "Modeling and control of satellite formations: A survey," *Automation*, vol. 3, p. 511–544, Sep 2022.

[4] G.-P. Liu and S. Zhang, "A survey on formation control of small satellites," *Proceedings of the IEEE*, vol. 106, no. 3, pp. 440–457, 2018.

[5] G. Inalhan, M. Tillerson, and J. P. How, "Relative dynamics and control of spacecraft formations in eccentric orbits," *Journal of guidance, control, and dynamics*, vol. 25, no. 1, pp. 48–59, 2002.

[6] D. P. Scharf, F. Y. Hadaegh, and S. R. Ploen, "A survey of spacecraft formation flying guidance and control. part ii: control," in *Proceedings of the 2004 American control conference*, vol. 4, pp. 2976–2985, Ieee, 2004.

[7] H. Zhang and P. Gurfil, "Satellite cluster flight using on-off cyclic control," *Acta Astronautica*, vol. 106, pp. 1–12, 2015.

[8] T. Villela, C. A. Costa, A. M. Brandão, F. T. Bueno, R. Leonardi, *et al.*, "Towards the thousandth cubesat: A statistical overview," *International Journal of Aerospace Engineering*, vol. 2019, 2019.

[9] D. Morgan, S.-J. Chung, L. Blackmore, B. Acikmese, D. Bayard, and F. Y. Hadaegh, "Swarm-keeping strategies for spacecraft under j2 and atmospheric drag perturbations," *Journal of Guidance, Control, and Dynamics*, vol. 35, no. 5, pp. 1492–1506, 2012.

[10] D. Krejci and P. Lozano, "Micro-machined ionic liquid electrospray thrusters for cubesat applications," in *Proceedings of the 35th International Electric Propulsion Conference*, pp. 1–14, Electric Rocket Propulsion Soc., 2017.

[11] K. Lemmer, "Propulsion for cubesats," *Acta Astronautica*, vol. 134, pp. 231–243, 2017.

[12] T. Roy, V. Hruby, N. Rosenblad, P. Rostler, and D. Spence, "Cubesat propulsion using electrospray thrusters," in *Small Satellite Conference*, 2009.

[13] F. Martel, L. Perna, and P. Lozano, "Miniature ion electrospray thrusters and performance test on cubesats," in *Small Satellite Conference*, 2012.

[14] A. Bemporad and C. Rocchi, "Decentralized linear time-varying model predictive control of a formation of unmanned aerial vehicles," in *2011 50th IEEE conference on decision and control and European control conference*, pp. 7488–7493, IEEE, 2011.

[15] Z. Cai, H. Zhou, J. Zhao, K. Wu, and Y. Wang, "Formation control of multiple unmanned aerial vehicles by event-triggered distributed model predictive control," *IEEE Access*, vol. 6, pp. 55614–55627, 2018.

[16] G. Franze, M. Mattei, L. Ollio, and V. Scordamaglia, "A robust constrained model predictive control scheme for norm-bounded uncertain systems with partial state measurements," *International Journal of Robust and Nonlinear Control*, vol. 29, no. 17, pp. 6105–6125, 2019.

[17] V. A. Nardi, A. Ferraro, and V. Scordamaglia, "Feasible trajectory planning algorithm for a skid-steered tracked mobile robot subject to skid and slip phenomena," in *2018 23rd International Conference on Methods & Models in Automation & Robotics (MMAR)*, pp. 120–125, IEEE, 2018.

[18] V. Scordamaglia, V. A. Nardi, and A. Ferraro, "A feasible trajectory planning algorithm for a network controlled robot subject to skid and slip phenomena," in *2019 24th IEEE International Conference on Emerging Technologies and Factory Automation (ETFA)*, pp. 933–940, IEEE, 2019.

[19] V. Scordamaglia and V. A. Nardi, "A set-based trajectory planning algorithm for a network controlled skid-steered tracked mobile robot subject to skid and slip phenomena," *Journal of Intelligent & Robotic Systems*, vol. 101, no. 1, p. 15, 2021.

[20] X. Zhang and R. Piche, "Application of the hill-clohessy-wiltshire equation in gnss orbit prediction," in *International Conference on Localization and GNSS 2014 (ICL-GNSS 2014)*, pp. 1–6, IEEE, 2014.

[21] W. Clohessy and R. Wiltshire, "Terminal guidance system for satellite rendezvous," *Journal of the Aerospace Sciences*, vol. 27, no. 9, pp. 653–658, 1960.

[22] O. Montenbruck and E. Gill, *Satellite Orbits Models, Methods and Applications*. Springer Berlin, Heidelberg, 2000.